Applied Surface Science 538 (2021) 148143

Contents lists available at ScienceDirect

Applied Surface Science

journal homepage: www.elsevier.com/locate/apsusc

Laser writing of $CsPbBr_3$ nanocrystals mediated by closely-packed Au nanoislands

Weijie Zhuang[a], Shulei Li[a], Fu Deng[a], Guangcan Li[a], Shaolong Tie[b], Sheng Lan[a,*]

[a] Guangdong Provincial Key Laboratory of Nanophotonic Functional Materials and Devices, School of Information and Optoelectronic Science and Engineering, South China Normal University, Guangzhou 510006, China

[b] School of Chemistry and Environment, South China Normal University, Guangzhou 510006, China

ARTICLE INFO

Keywords:
Perovskite nanocrystal
Gold nanoisland
Laser writing
Femtosecond laser pulse
Optical display

ABSTRACT

Metal halide perovskites have attracted great interest in recent years owing to their excellent luminescence properties. The low formation energy makes it possible to synthesize perovskites of different types via direct laser writing. Here, we report on the formation of metal halide perovskite ($CsPbBr_3$) nanocrystals coupled to the surface plasmon resonances of gold (Au) nanoparticles by irradiating a polymer film doped with the precursors (CsBr and $PbBr_3$) and coated on a thin Au film. The Au film, which is composed of closely-packed Au nanoislands deposited on a silica substrate, act as not only the absorber of 800-nm femtosecond laser pulses but also the heat source for synthesizing and annealing of $CsPbBr_3$ nanocrystals. The formation of $CsPbBr_3$ nanocrystals in the area of laser irradiation was confirmed by Raman scattering spectra measurements. In addition, closely-packed Au nanoislands are transformed into isolated Au nanoparticles which exhibit surface plasmon resonances at ~530 nm. The $CsPbBr_3$ nanocrystals coupled to isolated Au nanoparticles emit two-photon-induced luminescence at ~513 nm, which is enhanced by the surface plasmon resonances through the Purcell effect. An optimal laser power for direct laser writing was determined and the decomposition of $CsPbBr_3$ nanocrystals was observed if a large laser power was employed. Our results indicate the possibility for the formation and annealing of perovskite nanocrystals coupled to surface plasmon resonances by one-step laser writing and open new horizon for their practical applications in color display and optical memory.

1. Introduction

Metal halide perovskites have attracted great interest in recent years owing to their excellent electronic and optical properties, which have been widely applied in the fabrication of a variety of optoelectronic devices with high-performance, such as solar cells [1,2], light-emitting diodes [3–5], lasers [6,7], and optical sensors [8,9]. The simplicity of preparation and the low formation energy requirement [10,11] make it possible to prepare such perovskites with different compositions, morphologies, and sizes through colloidal chemical route for practical applications in various graphical scenes [12–15].

Recently, it was found that ultrashort pulse laser is a powerful tool to induce crystallization of functional micro- and nanocrystals in transparent materials [16,17]. It has been proved that the nonlinear absorption process induced by femtosecond laser pulses in a hybrid glass matrix can be employed to redistribute atoms in the laser focus region [18], leading to the migration of ions and local crystallization of perovskite nanocrystals in the glass matrix [14,15]. Although thermal accumulation effect can be realized by using femtosecond laser pulses with a high repetition rate [19,20], an additional heat treatment (or annealing) is necessary in order to produce luminescent perovskite nanocrystals. Therefore, generation of luminescent perovskite nanocrystals via one-step direct laser writing remains a challenge.

In this article, we proposed a novel strategy to produce luminescent $CsPbBr_3$ nanocrystals in a polymer film doped with the precursors via direct laser writing. A rough Au film composed of closely-packed Au nanoislands was employed to absorb effectively the photon energy of femtosecond laser light at 800 nm. The heat released from the melting of Au nanoislands was exploited for synthesizing and annealing $CsPbBr_3$ nanocrystals. The formation of $CsPbBr_3$ nanocrystals was confirmed by Raman scattering spectra measurements and they could emit efficiently two-photon-induced luminescence (TPL) under the excitation of femtosecond laser pulses. The emission of $CsPbBr_3$ nanocrystals was enhanced by the surface plasmon resonances of the thermally reshaped Au nanoparticles [21]. The decomposition of $CsPbBr_3$ nanocrystals was observed if the laser power was larger than the optimum value for laser

* Corresponding author.
E-mail address: slan@scnu.edu.cn (S. Lan).

https://doi.org/10.1016/j.apsusc.2020.148143
Received 14 August 2020; Received in revised form 10 September 2020; Accepted 9 October 2020
Available online 13 October 2020

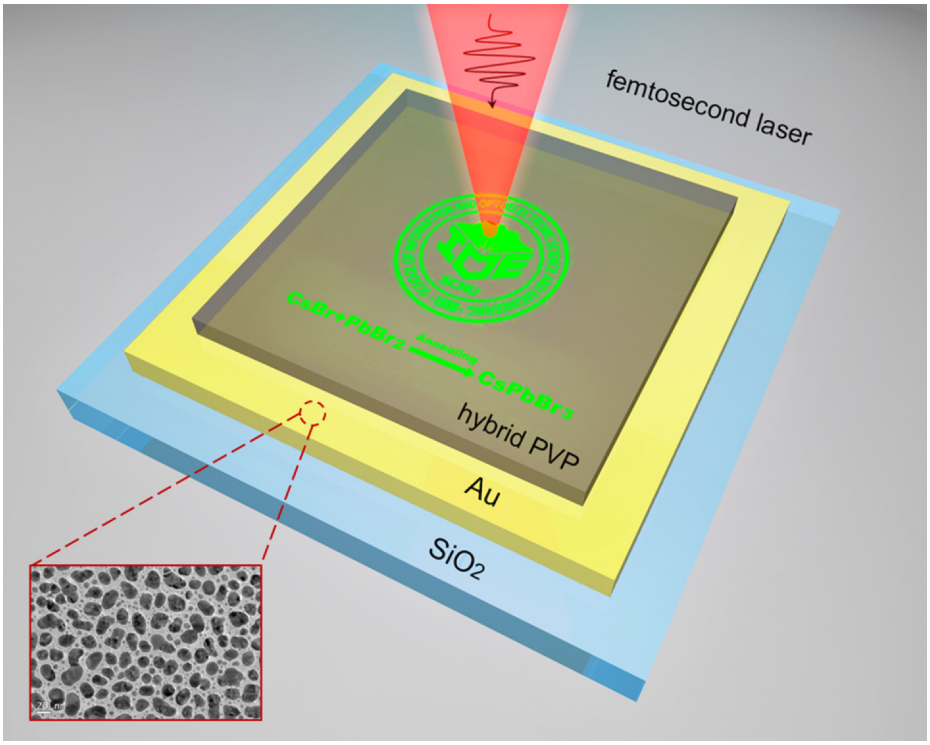

Fig. 1. Schematic illustrating the two-layer structure used for laser printing of $CsPbBr_3$ nanocrystals with focused femtosecond laser light. The morphology of the Au film, which is characterized by transmission electron microscope, is shown in the inset.

writing.

2. Materials and methods

2.1. Preparation of hybrid PVP film

CsBr and $PbBr_3$ powders with a molar ratio of 1:1 were weighed and dissolved into dimethyl sulfoxide (DMSO) uniformly with the help of a magnetic agitator. The solution was mixed with 100 mg/ml PVP and spin-coated on an Au film. The Au film was deposited on a silica (SiO_2) substrate by sputtering. The morphology of the Au film was controlled by the sputtering time. Based on the observation of transmission electron microscope, Au film composed of closely-packed Au nanoislands could be obtained by using a sputtering time of ~20 s. The PVP film doped with CsBr and $PbBr_3$ was dried under an infrared lamp.

2.2. Optical characterization

The femtosecond laser light with a wavelength of 800 nm, a repetition rate of 76 MHz and a duration of 130 fs (Mira 900S, Coherent) was employed for the laser writing of $CsPbBr_3$ nanocrystals. It was focused on the Au film beneath the hybrid PVP film by using the 60× objective lens (NA = 0.85) of a two-photon laser scanning confocal microscope (A1MP, Nikon) or an inverted luminescence microscope (Observer A1, Zeiss). The generated optical signals were collected by using the same objective lens and directed to a charge coupled device (DU970N, Andor) for imaging or to a spectrometer (SR-500i-B1, Andor) for analysis. The Raman scattering spectroscopy measurements were carried out with a Renishaw inVia instrument by using a 633-nm laser source.

2.3. Numerical modeling

The electric field distributions in two-dimensional closely-packed Au nanoislands and the temperature distributions in the array of randomly distributed Au nanoparticles were calculated numerically based on the finite element method (FEM) by using a commercially developed software (COMSOL Multiphysics v5.4). The smallest mesh size was chosen to be 1.0 nm. A perfectly matched layer boundary condition was employed to ensure the absorption of all the outgoing radiations. The temperature inside each Au nanoparticle was assumed to be uniform owing to the small size of nanoparticles and good conductivity of Au.

3. Results and discussion

3.1. Principle for laser writing of $CsPbBr_3$ nanocrystals

Although the formation energy of $CsPbBr_3$ is low, we still need to rise the temperature of the polymer film above a threshold in order to trigger the chemical reaction. For this reason, we intentionally chose a rough Au film instead of a flat one as the heat source for the polymer film. In addition, annealing of $CsPbBr_3$ nanocrystals needs to be completed at ambient temperature above 350 °C, which is also the key to realize laser writing of luminescent $CsPbBr_3$ nanocrystals [14]. Therefore, we need to find a way to increase the temperature of the polymer film, which facilitates the formation and annealing of $CsPbBr_3$ nanocrystals.

In Fig. 1, we show schematically the strategy employed to realize the laser writing of $CsPbBr_3$ nanocrystals. The polymer (PVP) film doped with CsBr and $PbBr_2$ was spin-coated on a thin Au film, which was beforehand deposited on a silica (SiO_2) substrate via sputtering. The Au film was composed of two-dimensional closely-packed Au nanoislands (see the inset of Fig. 1). Direct laser writing was performed by using a laser scanning confocal microscope equipped with a femtosecond laser light. The Au film was employed to absorb the photon energy of the femtosecond laser light. The heat released from the Au film was utilized to create $CsPbBr_3$ nanocrystals, which generate two-photon-induced luminescence (TPL) under the excitation of femtosecond laser pulses. Meanwhile, the Au nanoislands on the Au film were thermally

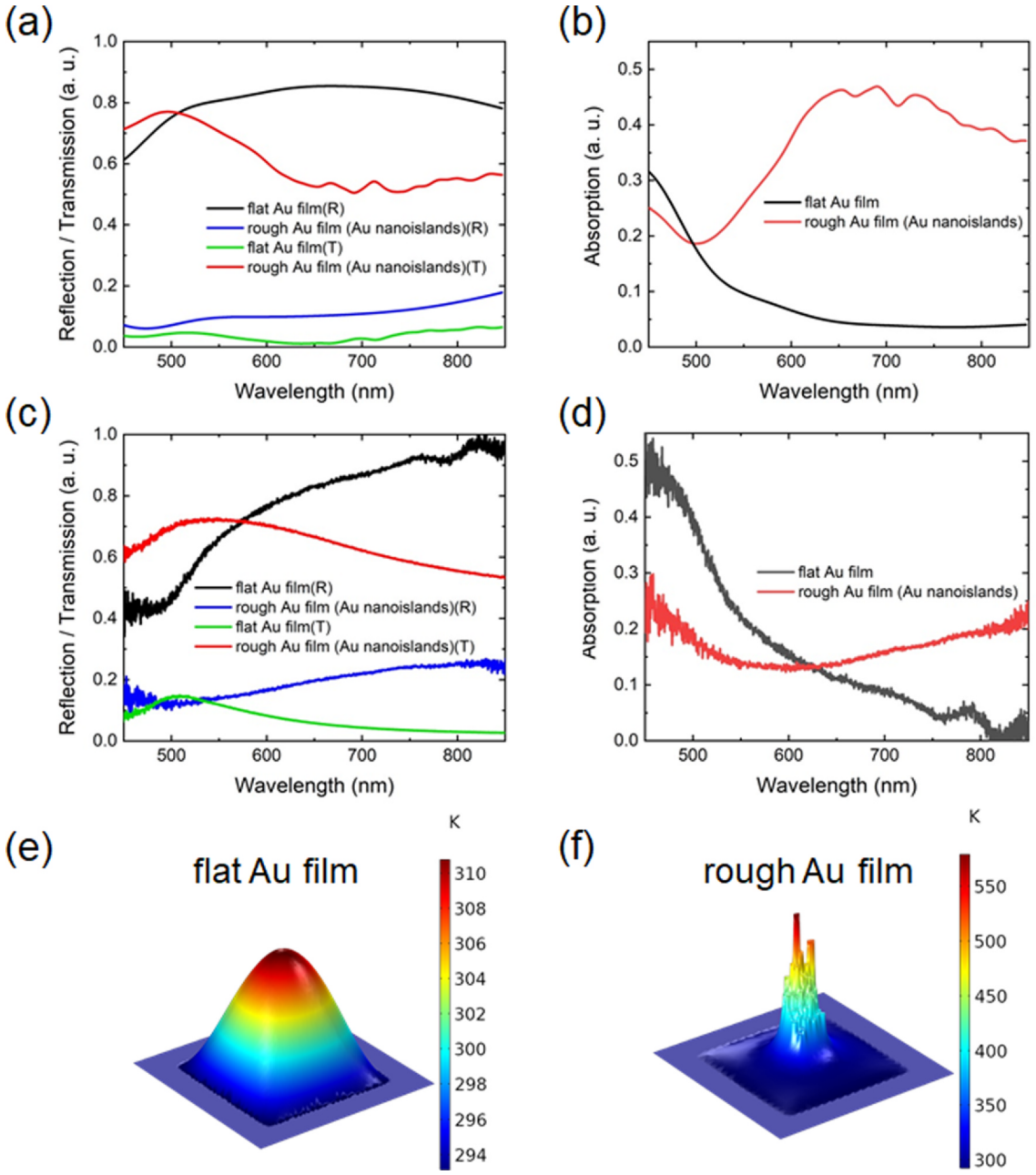

Fig. 2. Reflection and transmission spectra calculated (a) and measured (c) for the flat and rough Au films. The absorption spectra calculated and measured for the flat and rough Au films are shown in (b) and (d), respectively. The temperature distributions simulated for the flat and rough Au films are shown in (e) and (f), with an area of 500 × 500 nm^2.

reshaped by the femtosecond laser light and transformed into isolated Au nanoparticles. The surface plasmon resonances of the Au nanoparticles, which appear at ~530 nm, were exploited to enhance the emission rate of $CsPbBr_3$ nanocrystals.

3.2. Comparison of the absorptions and temperatures of flat and rough Au films

In Fig. 2a, we compare the reflection and transmission spectra simulated for a rough Au film and a flat one with the same thickness of 20 nm. The rough Au film was composed of two-dimensional closely-packed Au nanoislands and the transmission electron microscope (TEM) image of the film (see the inset of Fig. 1) was used to build the physical model for the numerical simulation. The absorption spectra of the rough and flat Au films derived from their reflection and transmission spectra are shown in Fig. 2b. In Fig. 2c and d, we compare the reflection/transmission and absorption spectra measured for the rough and flat Au films, respectively. It is remarkable that the absorption of the flat Au film at the wavelength of the femtosecond laser light (800 nm) is quite small (~5.0%). In sharp contrast, the absorption of the rough Au film, which was composed of closely-packed Au nanoislands, is increased by almost one order of magnitude (~40.0%). It implies that the photon energy of the femtosecond laser light can be efficiently absorbed by the rough Au film. In order to further confirm this point, we also simulated the temperature distributions in the polymer film induced by the two types of Au films irradiated by femtosecond laser light at 800 nm, as shown in Fig. 2e and f, respectively. It is found that the temperature rise induced by the rough Au film is much higher than that induced by the flat one, in good agreement with the absorption spectra calculated and measured for the two types of Au films.

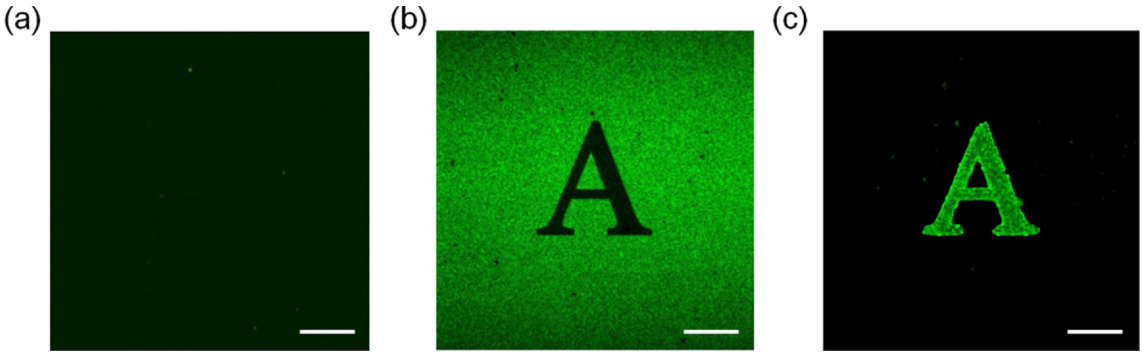

Fig. 3. Images obtained by scanning TPL of different structures with a laser scanning confocal microscope operating at 800 nm and 1 mW. In each case, a pattern (letter A) was beforehand recorded in the structure by using the laser scanning microscope with a larger laser power of 3 mW. (a) A polymer film doped with the precursors on a silica substrate. (b) A pure polymer film coated on a rough Au film. (c) A polymer film doped with the precursors and coated on a rough Au film. The length of the scale bars is 5 μm.

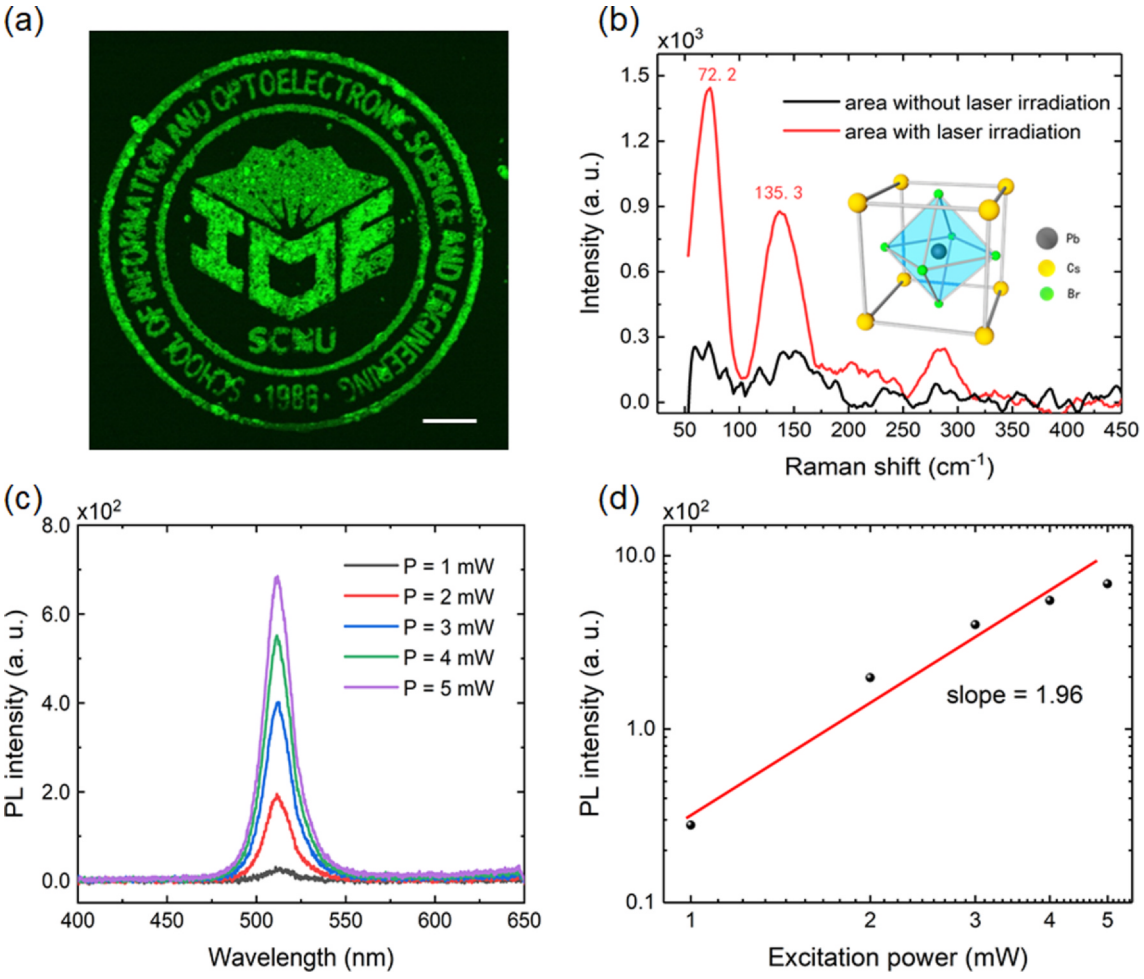

Fig. 4. (a) Image obtained by exciting and detecting the TPL of $CsPbBr_3$ nanoscrystals with a laser scanning confocal microscope operating at 800 nm and 1 mW. The school logo was beforehand recorded in the polymer film by using the laser scanning confocal microscope with a larger power of 3 mW. The length of the scale bar is 5.0 μm. (b) Raman scattering spectra measured for the areas without and with laser irradiation. (c) Luminescence spectra measured for $CsPbBr_3$ at different laser powers. (d) Dependence of the luminescence intensity on the excitation power plotted in a logarithmic coordinate.

3.3. Laser writing of $CsPbBr_3$ nanocrystals

In Fig. 3, we compare the images recorded in and extracted from different structures by using a laser scanning confocal microscope. For the polymer film doped with CsBr and $PbBr_2$ and coated on a SiO_2 substrate (without an Au film), only a dark background was observed, as shown in Fig. 3a. In this case, there is no heat supply necessary for the formation of $CsPbBr_3$ nanocrystals. In the pure polymer film coated on a rough Au film (see Fig. 3b), the recorded pattern (letter A) was observed because of the reduced TPL of the irradiated area as compared with the area without laser irradiation. However, the TPL in this case originates from Au nanoislands, which was reduced dramatically when Au nanoislands were thermally reshaped into isolated Au nanoparticles by femtosecond laser light. As a result, the surface plasmon resonances

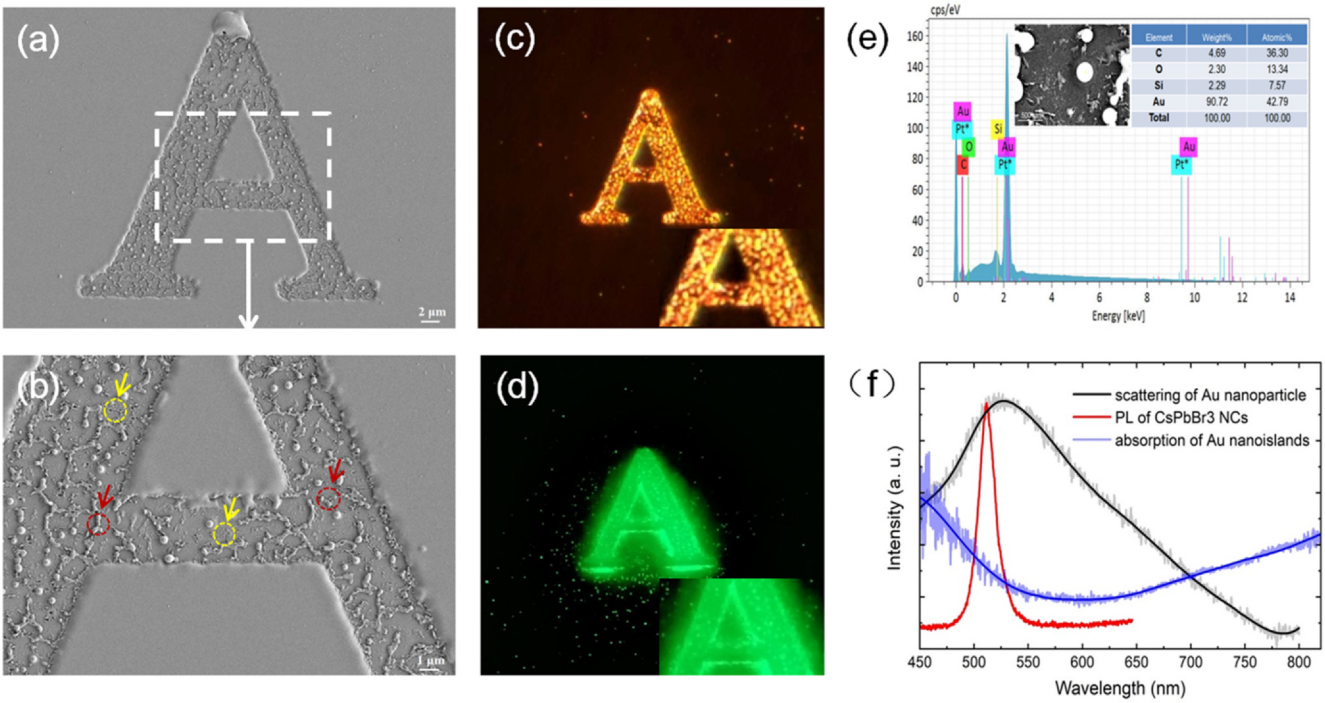

Fig. 5. (a) SEM image of the recorded pattern (letter A). (b) Magnified image of (a) in which Au nanoparticles with irregular shapes (red) and small diameters (yellow) are indicated by color arrows. (c) Dark-field microscope image of the recorded pattern. (d) Luminescent image of the recorded pattern excited by using a mercury lamp. (e) Energy dispersive X-ray spectrum measured for an Au nanoparticle. (f) Absorption spectrum measured for the rough Au film and the scattering spectrum measured for an isolated Au nanoparticle. The luminescence spectrum of $CsPbBr_3$ is also provided for reference.

were blueshifted to ~530 nm [22], leading to a weaker two-photon-induced absorption of the femtosecond laser light at 800 nm. In Fig. 3c, we show the pattern recorded in and extracted from a polymer film doped with the precursors and coated on a rough Au film. In contrast to the dark "A" observed in Fig. 3b, a bright "A" was revealed in this case, implying the formation of $CsPbBr_3$ nanocrystals. In addition, it indicates that the TPL emitted from $CsPbBr_3$ nanocrystals is much stronger than that from Au nanoislands.

3.4. Optical characterization of $CsPbBr_3$ nanocrystals

We have demonstrated that the formation of $CsPbBr_3$ nanocrystals can be realized by irradiating a polymer film doped with the precursors and coated on a rough Au film. The TPL of $CsPbBr_3$ nanocrystals appears to be much stronger than that of Au nanoislands under the excitation of femtosecond laser light. In Fig. 4a, we show a more complicated pattern (the logo of our school) recorded and extracted by using this method. It further confirms that the idea proposed in this work can be applied in optical color display and data storage. In order to confirm the formation of $CsPbBr_3$ nanocrystals, we also performed Raman spectroscopy characterization for the areas with and without laser irradiation, as shown in Fig. 4b. As compared with the area without laser irradiation, two strong Raman characteristic peaks located at 73 and 135 cm^{-1} were clearly resolved in the area with laser irradiation. These two scattering peaks can be attributed to the vibration modes of $[PbBr6]^{4-}$ octahedron and Cs^{+} cation movement [23,24], respectively. In comparison, the intensities of these two peaks are much weaker in the area of without laser irradiation. This result indicates undoubtedly that $CsPbBr_3$ nanocrystals were indeed created in the area irradiated by femtosecond laser light. In Fig. 4c, we show the luminescence spectra measured for $CsPbBr_3$ nanocrystals at different laser powers. As expected, the TPL of $CsPbBr_3$ nanocrystals appears as a single peak located at ~513 nm. A rapid increase of the luminescence is observed with increasing laser power. The linewidth of the emission band is estimated to be 15 nm, which is close to the value reported for bulk $CsPbBr_3$ [25]. It implies that the size of $CsPbBr_3$ nanocrystals is large and quantum confinement effect [26] is negligible in our case. A slope of ~1.96 is derived if we plot the luminescence intensity as a function of laser power in a logarithmic coordinate, as shown in Fig. 4d. The quadratic dependence of the luminescence intensity on laser power verifies the nature of the luminescence of $CsPbBr_3$ nanocrystals excited by femtosecond laser light at 800 nm [27,28].

3.5. $CsPbBr_3$ nanocrystals coupled to surface plasmon resonances

We examined the area with laser irradiation by using scanning electron microscope (SEM) observation, as shown in Fig. 5a. A magnified SEM image is presented in Fig. 5b. Many spherical nanoparticles can be found in the area with laser irradiation. It means that most Au nanoislands have been thermally melted and transformed into Au nanoparticles after absorbing the photon energy of femtosecond laser light. The formation of isolated Au nanoparticles in the area with laser irradiation can be clearly identified by using a dark-field microscope, as shown in Fig. 5c. Such Au nanoparticles appear as bright spots in the image owing to the stronger scattering of the white light used for illumination. Accordingly, such Au nanoparticles can also be resolved in the luminescence image excited by using the 365-nm line of a mercury lamp, as shown in Fig. 5d. It is because that the luminescence of $CsPbBr_3$ nanocrystals adjacent to Au nanoparticles is enhanced significantly by the surface plasmon resonances of Au nanoparticles, which are usually located at ~530 nm. Apart from large Au nanospheres, there are still some Au nanoparticles with irregular shapes and many small Au nanoparticles (as marked by arrows of different colors in Fig. 5b). Although the luminescence enhancement achieved for perovskite nanocrystals around these Au nanoparticles is not significant as compared with those around large Au nanospheres, the luminescence is still strong enough to clearly display the recorded pattern (see Fig. 5d). Based on energy dispersive X-ray spectroscopy (EDS), these nanoparticles were identified to be Au nanoparticles, as shown in Fig. 5e. In Fig. 5f, we present the scattering spectrum measured for an isolated Au

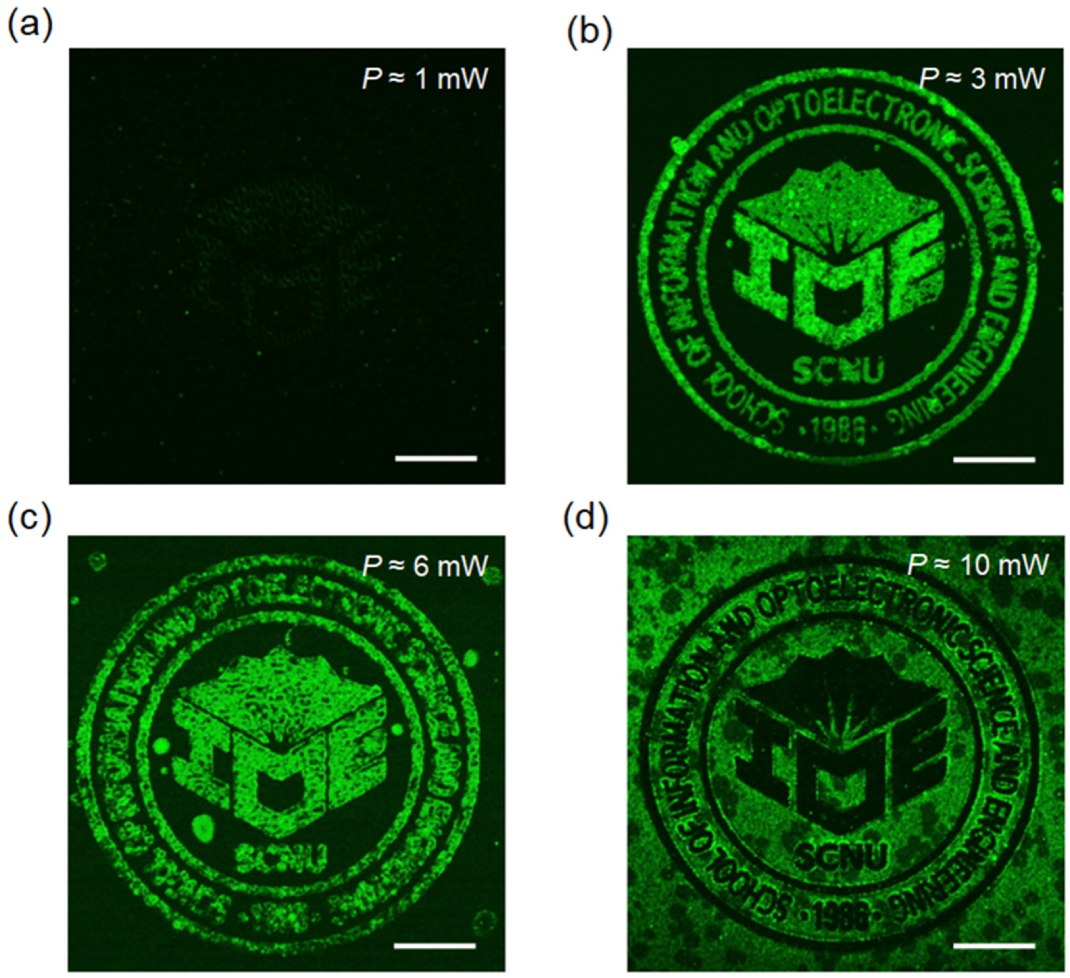

Fig. 6. Images obtained by exciting and detecting the TPL of $CsPbBr_3$ nanoscrystals with a laser scanning confocal microscope operating at 800 nm and 1 mW. The school logo was beforehand recorded in the polymer film with different laser powers. (a) P = 1.0 mW, (b) P = 3.0 mW, (c) P = 6.0 mW, and (d) P = 10.0 mW. In each case, the length of the scale bar is 50 μm.

nanoparticle. It appears as a broad band with a peak at ~530 nm. For comparison, we also present the absorption spectrum of the rough Au film, which shows a broad band with a large absorption at ~800 nm. Upon laser irradiation, the absorption peak is blue shifted to ~530 nm, providing luminescence enhancement for the generated $CsPbBr_3$ nanocrystals.

3.6. Photon-induced decomposition of $CsPbBr_3$ nanocrystals

In the laser writing of $CsPbBr_3$ nanocrystals demonstrated in this work, the laser power (P) used for direct writing is a key parameter because it determines the heat generation for the formation and annealing of $CsPbBr_3$ nanocrystals and also for the reshaping of Au nanoislands. In Fig. 6, we show the experimental results obtained by using different laser powers. The laser wavelength was fixed at 800 nm and the laser power used for readout was chosen to be 1 mW. For P = 1.0 mW, no luminescence contrast was detected and the recorded pattern was not successfully retrieved, as shown in Fig. 6a. It is thought that the heat generated by laser irradiation is not enough for the synthesis and annealing of $CsPbBr_3$ nanocrystals. When the laser power was increased to P = 3.0 mW, the heat generated by laser irradiation is sufficient for the formation of luminescent $CsPbBr_3$ nanocrystals. As a result, the recorded pattern can be extracted by detecting the TPL of $CsPbBr_3$ nanocrystals. As the laser power was further raised to P = 6.0 mW, the extracted pattern was deteriorated. In this case, the details become blurred and the area without laser irradiation also exhibits fluorescence response, as shown in Fig. 6c. This phenomenon arises from the diffusion of the heat, which has a significant impact on the integrity and clarity of the extracted pattern. Surprisingly, the extracted pattern was reversed when a large laser power of P = 10.0 mW was employed, as shown in Fig. 6d. In this case, the extracted pattern appeared to be dark, similar to that observed in Fig. 3b. This behavior was also observed in the laser writing of $CsPbBr_3$ quantum dots in glass matrix [14]. It can be attributed to the decomposition of $CsPbBr_3$ nanoscrystals induced by photon excitation, which quenches the luminescence.

The generation of luminescent perovskite nanocrystals includes the synthesis and annealing processes which need the heat released by Au nanoislands after absorbing the femtosecond laser light. Therefore, we think that luminescent perovskite nanocrystals are preferentially created around the hot spots formed by closely-packed Au nanoislands through plasmonic coupling. At low laser powers, only the Au nanoislands around the hot spots are melted because of the larger absorption efficiencies. In comparison, all the Au nanoislands will be melted and reshaped at high laser powers. In addition, the photon-induced decomposition of $CsPbBr_3$, which leads to the quenching of the luminescence, needs to be taken into account. Thus, it is difficult to estimate the concentration of the luminescent perovskite nanocrystals, which depends strongly on the laser power. Basically, the enhancement of the luminescence depends strongly on the distance between perovskite nanocrystals and Au nanoparticles. Based on previous studies, it has been known that the luminescence of a photon emitter (e.g., molecules or quantum dots) will be enhanced by a plasmonic nanoparticle

provided that the distance between them is larger than ~5 nm. Otherwise, the luminescence will be quenched. The enhancement factor decreases rapidly with increasing distance and it almost disappears for distances larger than ~25 nm. Therefore, we think that the enhancement of luminescence can only be achieved for perovskite nanocrystals whose distances to Au nanoparticles range from ~5 to ~25 nm.

4. Conclusion

In summary, we have successfully demonstrated that the laser writing of $CsPbBr_3$ nanocrystals can be realized by irradiating a polymer film doped with the precursors with femtosecond laser light. The polymer film was supported by using a rough Au film composed of Au nanoislands, which absorb efficiently the photon energy of femtosecond laser light. It was found that the heat released by the Au film is sufficient for synthesis and annealing of $CsPbBr_3$ nanocrystals and thus the generation of luminescent $CsPbBr_3$ nanocrystals can be completed via one-step direct laser writing. The formation of $CsPbBr_3$ nanocrystals in the area of laser irradiation was confirmed by Raman scattering spectroscopy measurements and the luminescence emitted from $CsPbBr_3$ nanocrystals was verified to be TPL. It was revealed that Au nanoislands were reshaped into isolated Au nanonarptices with surface plasmon resonances at ~530 nm. As a result, the luminescence of $CsPbBr_3$ nanocrystals adjacent to Au nanoparticles was greatly enhanced. Finally, an optimal laser power for laser writing was determined and the decomposition of $CsPbBr_3$ nanocrystals was observed if a large laser power was employed in laser writing. Our findings provide an effective way of synthesizing luminescent $CsPbBr_3$ nanocrystals for practical applications in color display and optical memory.

Author contribution

S. Lan. and W. Zhuang conceived the idea. W. Zhuang, S. Li, F. Deng and G. Li carried out the optical measurements and numerical simulations. S. Lan., W. Zhuang, S. Tie analyzed the data and wrote the manuscript. S. Lan and S. Tie supervised the project. All the authors read and commented on the manuscript.

Declaration of Competing Interest

The authors declare that they have no known competing financial interests or personal relationships that could have appeared to influence the work reported in this paper.

Acknowledgements

This work was financially supported by the National Natural and Science Foundation of China (Grant Nos. 11674110 and 11874020), the Natural Science Foundation of Guangdong Province, China (Grant Nos. 2016A030308010), and the Science and Technology Planning Project of Guangdong Province, China (Grant No. 2015B090927006).

.

References

[1] N.J. Jeon, H. Na, E.H. Jung, T.-Y. Yang, Y.G. Lee, G. Kim, H.-W. Shin, S. Il Seok, J. Lee, J. Seo, A fluorene-terminated hole-transporting material for highly efficient and stable perovskite solar cells, Nature Energy 3 (2018) 682–689.

[2] E.H. Jung, N.J. Jeon, E.Y. Park, C.S. Moon, T.J. Shin, T.Y. Yang, J.H. Noh, J. Seo, Efficient, stable and scalable perovskite solar cells using poly(3-hexylthiophene), Nature 567 (2019) 511–515.

[3] Z. Li, Z. Chen, Y. Yang, Q. Xue, H.L. Yip, Y. Cao, Modulation of recombination zone position for quasi-two-dimensional blue perovskite light-emitting diodes with efficiency exceeding 5, Nat. Commun. 10 (2019) 1027.

[4] K. Lin, J. Xing, L.N. Quan, F.P.G. de Arquer, X. Gong, J. Lu, L. Xie, W. Zhao, D. Zhang, C. Yan, W. Li, X. Liu, Y. Lu, J. Kirman, E.H. Sargent, Q. Xiong, Z. Wei, Perovskite light-emitting diodes with external quantum efficiency exceeding 20 per cent, Nature 562 (2018) 245–248.

[5] L. Zhao, Y.W. Yeh, N.L. Tran, F. Wu, Z. Xiao, R.A. Kerner, Y.L. Lin, G.D. Scholes, N. Yao, B.P. Rand, In situ preparation of metal halide perovskite nanocrystal thin films for improved light-emitting devices, ACS Nano 11 (2017) 3957–3964.

[6] Y. Jia, R.A. Kerner, A.J. Grede, B.P. Rand, N.C. Giebink, Continuous-wave lasing in an organic–inorganic lead halide perovskite semiconductor, Nat. Photon. 11 (2017) 784–788.

[7] B. Tang, H. Dong, L. Sun, W. Zheng, Q. Wang, F. Sun, X. Jiang, A. Pan, L. Zhang, Single-mode lasers based on cesium lead halide perovskite submicron spheres, ACS Nano 11 (2017) 10681–10688.

[8] H. Gao, J. Feng, Y. Pi, Z. Zhou, B. Zhang, Y. Wu, X. Wang, X. Jiang, L. Jiang, Bandgap engineering of single-crystalline perovskite arrays for high-performance photodetectors, Adv. Funct. Mater. 28 (2018).

[9] Q. Chen, J. Wu, X. Ou, B. Huang, J. Almutlaq, A.A. Zhumekenov, X. Guan, S. Han, L. Liang, Z. Yi, J. Li, X. Xie, Y. Wang, Y. Li, D. Fan, D.B.L. Teh, A.H. All, O.F. Mohammed, O.M. Bakr, T. Wu, M. Bettinelli, H. Yang, W. Huang, X. Liu, All-inorganic perovskite nanocrystal scintillators, Nature 561 (2018) 88–93.

[10] L. Protesescu, S. Yakunin, M.I. Bodnarchuk, F. Krieg, R. Caputo, C.H. Hendon, R.X. Yang, A. Walsh, M.V. Kovalenko, Nanocrystals of cesium lead halide perovskites (CsPbX(3), X = Cl, Br, and I): novel optoelectronic materials showing bright emission with wide color gamut, Nano Lett. 15 (2015) 3692–3696.

[11] S. Zou, Y. Liu, J. Li, C. Liu, R. Feng, F. Jiang, Y. Li, J. Song, H. Zeng, M. Hong, X. Chen, Stabilizing cesium lead halide perovskite lattice through Mn(II) substitution for air-stable light-emitting diodes, J. Am. Chem. Soc. 139 (2017) 11443–11450.

[12] Y. Liu, F. Li, L. Qiu, K. Yang, Q. Li, X. Zheng, H. Hu, T. Guo, C. Wu, T.W. Kim, Fluorescent microarrays of in situ crystallized perovskite nanocomposites fabricated for patterned applications by using inkjet printing, ACS Nano 13 (2019) 2042–2049.

[13] D.N. Minh, S. Eom, L.A.T. Nguyen, J. Kim, J.H. Sim, C. Seo, J. Nam, S. Lee, S. Suk, J. Kim, Y. Kang, Perovskite nanoparticle composite films by size exclusion lithography, Adv. Mater. 30 (2018) e1802555.

[14] X. Huang, Q. Guo, D. Yang, X. Xiao, X. Liu, Z. Xia, F. Fan, J. Qiu, G. Dong, Reversible 3D laser printing of perovskite quantum dots inside a transparent medium, Nat. Photon. 14 (2019) 82–88.

[15] X. Huang, Q. Guo, S. Kang, T. Ouyang, Q. Chen, X. Liu, Z. Xia, Z. Yang, Q. Zhang, J. Qiu, G. Dong, Three-dimensional laser-assisted patterning of blue-emissive metal halide perovskite nanocrystals inside a glass with switchable photoluminescence, ACS Nano 14 (2020) 3150–3158.

[16] D. Wei, C. Wang, H. Wang, X. Hu, D. Wei, X. Fang, Y. Zhang, D. Wu, Y. Hu, J. Li, S. Zhu, M. Xiao, Experimental demonstration of a three-dimensional lithium niobate nonlinear photonic crystal, Nat. Photon. 12 (2018) 596–600.

[17] T. Xu, K. Switkowski, X. Chen, S. Liu, K. Koynov, H. Yu, H. Zhang, J. Wang, Y. Sheng, W. Krolikowski, Three-dimensional nonlinear photonic crystal in ferroelectric barium calcium titanate, Nat. Photon. 12 (2018) 591–595.

[18] T.T. Fernandez, M. Sakakura, S.M. Eaton, B. Sotillo, J. Siegel, J. Solis, Y. Shimotsuma, K. Miura, Bespoke photonic devices using ultrafast laser driven ion migration in glasses, Prog. Mater Sci. 94 (2018) 68–113.

[19] M. Shimizu, M. Sakakura, M. Ohnishi, Y. Shimotsuma, T. Nakaya, K. Miura, K. Hirao, Mechanism of heat-modification inside a glass after irradiation with high-repetition rate femtosecond laser pulses, J. Appl. Phys. 108 (2010).

[20] H. Li, X.-F. Li, C.-Y. Zhang, S.-L. Tie, S. Lan, Narrow titanium oxide nanowires induced by femtosecond laser pulses on a titanium surface, Appl. Surf. Sci. 396 (2017) 221–225.

[21] S. Bishnoi, R. Das, S. Chawla, Gold nanosphere enhanced green and red fluorescence in ZnO: Al, Eu3+, Appl. Phys. Lett. 105 (2014).

[22] J.D. Chen, J. Xiang, S. Jiang, Q.F. Dai, S.L. Tie, S. Lan, Radiation of the high-order plasmonic modes of large gold nanospheres excited by surface plasmon polaritons, Nanoscale 10 (2018) 9153–9163.

[23] O. Yaffe, Y. Guo, L.Z. Tan, D.A. Egger, T. Hull, C.C. Stoumpos, F. Zheng, T.F. Heinz, L. Kronik, M.G. Kanatzidis, J.S. Owen, A.M. Rappe, M.A. Pimenta, L.E. Brus, Local polar fluctuations in lead halide perovskite crystals, Phys. Rev. Lett. 118 (2017) 136001.

[24] J.H. Cha, J.H. Han, W. Yin, C. Park, Y. Park, T.K. Ahn, J.H. Cho, D.Y. Jung, Photoresponse of CsPbBr 3 and Cs4PbBr6 perovskite single crystals, J. Phys. Chem. Lett. 8 (2017) 565–570.

[25] B. Zhou, M. Jiang, H. Dong, W. Zheng, Y. Huang, J. Han, A. Pan, L. Zhang, High-temperature upconverted single-mode lasing in 3D fully inorganic perovskite microcubic cavity, ACS Photon. 6 (2019) 793–801.

[26] Z. Liang, S. Zhao, Z. Xu, B. Qiao, P. Song, D. Gao, X. Xu, Shape-Controlled synthesis of all-inorganic $CsPbBr_3$ perovskite nanocrystals with bright blue emission, ACS Appl. Mater. Interf. 8 (2016) 28824–28830.

[27] K. Wei, Z. Xu, R. Chen, X. Zheng, X. Cheng, T. Jiang, Temperature-dependent excitonic photoluminescence excited by two-photon absorption in perovskite $CsPbBr_3$ quantum dots, Opt. Lett. 41 (2016) 3821–3824.

[28] Y. Wang, X. Li, X. Zhao, L. Xiao, H. Zeng, H. Sun, Nonlinear absorption and low-threshold multiphoton pumped stimulated emission from all-inorganic perovskite nanocrystals, Nano Lett. 16 (2016) 448–453.